Chapter 2

Central-Field Schrödinger Equation

We begin the present discussion with a review of the Schrödinger equation for a single electron in a central potential $V(r)$. First, we decompose the Schrödinger wave function in spherical coordinates and set up the equation governing the radial wave function. Following this, we consider analytical solutions to the radial Schrödinger equation for the special case of a Coulomb potential. The analytical solutions provide a guide for our later numerical analysis. This review of basic quantum mechanics is followed by a discussion of the numerical solution to the radial Schrödinger equation.

The single-electron Schrödinger equation is used to describe the electronic states of an atom in the independent-particle approximation, a simple approximation for a many-particle system in which each electron is assumed to move independently in a potential that accounts for the nuclear field and the field of the remaining electrons. There are various methods for determining an approximate potential. Among these are the Thomas-Fermi theory and the Hartree-Fock theory, both of which will be taken up later. In the following section, we assume that an appropriate central potential has been given and we concentrate on solving the resulting single-particle Schrödinger equation.

2.1 Radial Schrödinger Equation

First, we review the separation in spherical coordinates of the Schrödinger equation for an electron moving in a central potential $V(r)$. We assume that $V(r) = V_{\rm nuc}(r) + U(r)$ is the sum of a nuclear potential

$$V_{\rm nuc}(r) = -\frac{Ze^2}{4\pi\epsilon_0}\frac{1}{r} \ ,$$

and an average potential $U(r)$ approximating the electron-electron interaction.

We let $\psi(\mathbf{r})$ designate the single-particle wave function. In the sequel, we refer to this wave function as an *orbital* to distinguish it from a many-particle wave function. The orbital $\psi(\mathbf{r})$ satisfies the Schrödinger equation

$$h\psi = E\psi \,, \tag{2.1}$$

where the Hamiltonian h is given by

$$h = \frac{p^2}{2m} + V(r) \,. \tag{2.2}$$

In Eq.(2.2), $\mathbf{p} = -i\hbar\boldsymbol{\nabla}$ is the momentum operator and m is the electron's mass. The Schrödinger equation, when expressed in spherical coordinates, (r, θ, ϕ), becomes

$$\begin{aligned} &\frac{1}{r^2}\frac{\partial}{\partial r}\left(r^2\frac{\partial\psi}{\partial r}\right) + \frac{1}{r^2\sin\theta}\frac{\partial}{\partial\theta}\left(\sin\theta\frac{\partial\psi}{\partial\theta}\right) \\ &+\frac{1}{r^2\sin^2\theta}\frac{\partial^2\psi}{\partial\phi^2} + \frac{2m}{\hbar^2}\left(E - V(r)\right)\psi = 0 \,. \end{aligned} \tag{2.3}$$

We seek a solution $\psi(r, \theta, \phi)$ that can be expressed as a product of a function P of r only, and a function Y of the angles θ and ϕ:

$$\psi(\mathbf{r}) = \frac{1}{r}P(r)\,Y(\theta, \phi) \,. \tag{2.4}$$

Substituting this *ansatz* into Eq.(2.3), we obtain the following pair of equations for the functions P and Y

$$\frac{1}{\sin\theta}\frac{\partial}{\partial\theta}\left(\sin\theta\frac{\partial Y}{\partial\theta}\right) + \frac{1}{\sin^2\theta}\frac{\partial^2 Y}{\partial\phi^2} + \lambda Y = 0 \,, \tag{2.5}$$

$$\frac{d^2P}{dr^2} + \frac{2m}{\hbar^2}\left(E - V(r) - \frac{\lambda\hbar^2}{2mr^2}\right)P = 0 \,, \tag{2.6}$$

where λ is an arbitrary separation constant.

If we set $\lambda = \ell(\ell+1)$, where $\ell = 0,\ 1,\ 2,\ \cdots$ is an integer, then the solutions to Eq.(2.5) that are finite and single valued for all angles are the spherical harmonics $Y_{\ell m}(\theta, \phi)$.

The normalization condition for the wave function $\psi(\mathbf{r})$ is

$$\int d^3r\psi^\dagger(\mathbf{r})\psi(\mathbf{r}) = 1 \,, \tag{2.7}$$

which leads to normalization condition

$$\int_0^\infty dr\, P^2(r) = 1 \,, \tag{2.8}$$

for the radial function $P(r)$.

The expectation value $\langle O \rangle$ of an operator O in the state ψ is given by

$$\langle O \rangle = \int d^3 r \psi^\dagger(\mathbf{r}) O \psi(\mathbf{r}) \,. \tag{2.9}$$

In the state described by $\psi(\mathbf{r}) = \frac{P(r)}{r} Y_{\ell m}(\theta, \phi)$, we have

$$\langle L^2 \rangle = \ell(\ell+1)\hbar^2 \,, \tag{2.10}$$

$$\langle L_z \rangle = m\hbar \,. \tag{2.11}$$

2.2 Coulomb Wave Functions

The basic equation for our subsequent numerical studies is the radial Schrödinger equation (2.6) with the separation constant $\lambda = \ell(\ell+1)$:

$$\frac{d^2 P}{dr^2} + \frac{2m}{\hbar^2}\left(E - V(r) - \frac{\ell(\ell+1)\hbar^2}{2mr^2}\right) P = 0 \,. \tag{2.12}$$

We start our discussion of this equation by considering the special case $V(r) = V_{\rm nuc}(r)$.

Atomic Units: Before we start our analysis, it is convenient to introduce atomic units in order to rid the equation of unnecessary physical constants. Atomic units are defined by requiring that the electron's mass m, the electron's charge $|e|/\sqrt{4\pi\epsilon_0}$, and Planck's constant $\hbar$, all have the value 1. The atomic unit of length is the Bohr radius, $a_0 = 4\pi\epsilon_0\hbar^2/me^2 = 0.529177\ldots$ Å, and the atomic unit of energy is $me^4/(4\pi\epsilon_0\hbar)^2 = 27.2114\ldots$ eV. Units for other quantities can be readily worked out from these basic few. For example, the atomic unit of velocity is $c\alpha$, where c is the speed of light and α is Sommerfeld's fine structure constant: $\alpha = e^2/4\pi\epsilon_0\hbar c = 1/137.0359895\ldots$.

In atomic units, Eq.(2.12) becomes

$$\frac{d^2 P}{dr^2} + 2\left(E + \frac{Z}{r} - \frac{\ell(\ell+1)}{2r^2}\right) P = 0 \,. \tag{2.13}$$

We seek solutions to the radial Schrödinger equation (2.13) that satisfy the normalization condition (2.8). Such solutions exist only for certain discrete values of the energy, $E = E_{n\ell}$, the energy eigenvalues. Our problem is to determine these energy eigenvalues and the associated eigenfunctions, $P_{n\ell}(r)$. If we have two eigenfunctions, $P_{n\ell}(r)$ and $P_{m\ell}(r)$, belonging to the same angular momentum quantum number ℓ but to distinct eigenvalues, $E_{m\ell} \neq E_{n\ell}$, then it follows from Eq.(2.13) that

$$\int_0^\infty dr P_{n\ell}(r) P_{m\ell}(r) = 0 \,. \tag{2.14}$$

Near $r = 0$, solutions to Eq.(2.13) take on one of the following limiting forms:

$$P(r) \to \begin{cases} r^{\ell+1} & \text{regular at the origin, or} \\ r^{-\ell} & \text{irregular at the origin} \end{cases} . \tag{2.15}$$

Since we seek normalizable solutions, we must require that our solutions be of the first type, regular at the origin. The desired solution grows as $r^{\ell+1}$ as r moves outward from the origin while the complementary solution decreases as $r^{-\ell}$ as r increases.

Since the potential vanishes as $r \to \infty$, it follows that

$$P(r) \to \begin{cases} e^{-\lambda r} & \text{regular at infinity, or} \\ e^{\lambda r} & \text{irregular at infinity} \end{cases} , \tag{2.16}$$

where $\lambda = \sqrt{-2E}$. Again, the normalizability constraint (2.8) forces us to seek solutions of the first type, regular at infinity. Substituting

$$P(r) = r^{\ell+1} e^{-\lambda r} F(r) \tag{2.17}$$

into Eq.(2.13), we find that $F(x)$ satisfies Kummer's equation

$$x \frac{d^2F}{dx^2} + (b - x)\frac{dF}{dx} - aF = 0 , \tag{2.18}$$

where $x = 2\lambda r$, $a = \ell + 1 - Z/\lambda$, and $b = 2(\ell+1)$. The solutions to Eq.(2.18) that are regular at the origin are the Confluent Hypergeometric functions (Magnus and Oberhettinger, 1949, chap. VI):

$$\begin{aligned} F(a,b,x) &= 1 + \frac{a}{b}x + \frac{a(a+1)}{b(b+1)}\frac{x^2}{2!} + \frac{a(a+1)(a+2)}{b(b+1)(b+2)}\frac{x^3}{3!} + \cdots \\ &+ \frac{a(a+1)\cdots(a+k-1)}{b(b+1)\cdots(b+k-1)}\frac{x^k}{k!} + \cdots . \end{aligned} \tag{2.19}$$

This series has the asymptotic behavior

$$F(a,b,x) \to \frac{\Gamma(b)}{\Gamma(a)}\, e^x x^{a-b}[1 + O(|x|^{-1})] , \tag{2.20}$$

for large $|x|$. The resulting radial wave function, therefore, grows exponentially unless the coefficient of the exponential in Eq.(2.20) vanishes. Since $\Gamma(b) \neq 0$, we must require $\Gamma(a) = \infty$ to obtain normalizable solutions. The function $\Gamma(a) = \infty$ when a vanishes or when a is a negative integer. Thus, normalizable wave functions are only possible when $a = -n_r$ with $n_r = 0, 1, 2, \cdots$. The quantity n_r is called the radial quantum number. With $a = -n_r$, the Confluent Hypergeometric function in Eq.(2.19) reduces to a polynomial of degree n_r. The integer n_r equals the number of nodes (zeros) of the radial wave function for $r > 0$. From $a = \ell + 1 - Z/\lambda$, it follows that

$$\lambda = \lambda_n = \frac{Z}{n_r + \ell + 1} = \frac{Z}{n} ,$$

with $n = n_r + \ell + 1$. The positive integer n is called the principal quantum number. The relation $\lambda = \sqrt{-2E}$ leads immediately to the energy eigenvalue equation

$$E = E_n = -\frac{\lambda_n^2}{2} = -\frac{Z^2}{2n^2} \, . \tag{2.21}$$

There are n distinct radial wave functions corresponding to E_n. These are the functions $P_{n\ell}(r)$ with $\ell = 0, 1, \cdots, n-1$. The radial function is, therefore, given by

$$P_{n\ell}(r) = N_{n\ell} \, (2Zr/n)^{\ell+1} e^{-Zr/n} F(-n+\ell+1, 2\ell+2, 2Zr/n) \, , \tag{2.22}$$

where $N_{n\ell}$ is a normalization constant. This constant is determined by requiring

$$N_{n\ell}^2 \int_0^\infty dr \, (2Zr/n)^{2\ell+2} e^{-2Zr/n} F^2(-n+\ell+1, 2\ell+2, 2Zr/n) = 1 \, . \tag{2.23}$$

This integral can be evaluated analytically to give

$$N_{n\ell} = \frac{1}{n(2\ell+1)!} \sqrt{\frac{Z(n+\ell)!}{(n-\ell-1)!}} \, . \tag{2.24}$$

The radial functions $P_{n\ell}(r)$ for the lowest few states are found to be:

$$P_{10}(r) = 2Z^{3/2} \, r e^{-Zr} \, , \tag{2.25}$$

$$P_{20}(r) = \frac{1}{\sqrt{2}} Z^{3/2} \, r e^{-Zr/2} \left(1 - \frac{1}{2} Zr\right) \, , \tag{2.26}$$

$$P_{21}(r) = \frac{1}{2\sqrt{6}} Z^{5/2} \, r^2 e^{-Zr/2} \, , \tag{2.27}$$

$$P_{30}(r) = \frac{2}{3\sqrt{3}} Z^{3/2} \, r e^{-Zr/3} \left(1 - \frac{2}{3} Zr + \frac{2}{27} Z^2 r^2\right) \, , \tag{2.28}$$

$$P_{31}(r) = \frac{8}{27\sqrt{6}} Z^{5/2} \, r^2 e^{-Zr/3} \left(1 - \frac{1}{6} Zr\right) \, , \tag{2.29}$$

$$P_{32}(r) = \frac{4}{81\sqrt{30}} Z^{7/2} \, r^3 e^{-Zr/3} . \tag{2.30}$$

In Fig. 2.1, we plot the Coulomb wave functions for the $n = 1$, 2 and 3 states of hydrogen, $Z = 1$. In this figure, the angular momentum states are labeled using spectroscopic notation: states with $l = 0, 1, 2, 3, 4, \cdots$ are given the labels $s, p, d, f, g, \cdots$, respectively. It should be noted that the radial functions with the lowest value of l for a given n, have no nodes for $r > 0$, corresponding to the fact that $n_r = 0$ for such states. The number of nodes is seen to increase in direct proportion to n for a fixed value of l. The outermost maximum of each wave function is seen to occur at increasing distances from the origin as n increases.

The expectation values of powers of r, given by

$$\langle r^\nu \rangle_{n\ell} = N_{n\ell}^2 \left(\frac{n}{2Z}\right)^{\nu+1} \int_0^\infty dx \, x^{2\ell+2+\nu} e^{-x} F^2(-n+\ell+1, 2\ell+2, x) \, , \tag{2.31}$$

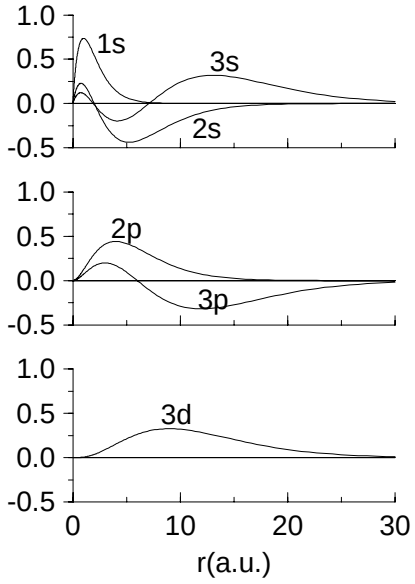

Figure 2.1: Hydrogenic Coulomb wave functions for states with $n = 1$, 2 and 3.

can be evaluated analytically. One finds:

$$\langle r^2\rangle_{n\ell} = \frac{n^2}{2Z^2}[5n^2 + 1 - 3\ell(\ell+1)]\,, \tag{2.32}$$

$$\langle r\rangle_{n\ell} = \frac{1}{2Z}[3n^2 - \ell(\ell+1)]\,, \tag{2.33}$$

$$\left\langle \frac{1}{r}\right\rangle_{n\ell} = \frac{Z}{n^2}\,, \tag{2.34}$$

$$\left\langle \frac{1}{r^2}\right\rangle_{n\ell} = \frac{Z^2}{n^3(\ell+1/2)}\,, \tag{2.35}$$

$$\left\langle \frac{1}{r^3}\right\rangle_{n\ell} = \frac{Z^3}{n^3(\ell+1)(\ell+1/2)\ell}\,, \quad \ell > 0\,, \tag{2.36}$$

$$\left\langle \frac{1}{r^4}\right\rangle_{n\ell} = \frac{Z^4[3n^2 - \ell(\ell+1)]}{2n^5(\ell+3/2)(\ell+1)(\ell+1/2)\ell(\ell-1/2)}\,, \quad \ell > 0\,. \tag{2.37}$$

These formulas follow from the expression for the expectation value of a power of r given by Bethe and Salpeter (1957):

$$\langle r^\nu\rangle = \left(\frac{n}{2Z}\right)^\nu \frac{J^{(\nu+1)}_{n+l,2l+1}}{J^{(1)}_{n+l,2l+1}}\,, \tag{2.38}$$

where, for $\sigma \geq 0$,

$$J^{(\sigma)}_{\lambda,\mu} = (-1)^{\sigma} \frac{\lambda!\,\sigma!}{(\lambda-\mu)!} \sum_{\beta=0}^{\sigma} (-1)^{\beta} \begin{pmatrix} \sigma \\ \beta \end{pmatrix} \begin{pmatrix} \lambda+\beta \\ \sigma \end{pmatrix} \begin{pmatrix} \lambda+\beta-\mu \\ \sigma \end{pmatrix}, \quad (2.39)$$

and for $\sigma = -(s+1) \leq -1$,

$$J^{(\sigma)}_{\lambda,\mu} = \frac{\lambda!}{(\lambda-\mu)!\,(s+1)!} \sum_{\gamma=0}^{s} (-1)^{s-\gamma} \frac{\begin{pmatrix} s \\ \gamma \end{pmatrix} \begin{pmatrix} \lambda-\mu+\gamma \\ s \end{pmatrix}}{\begin{pmatrix} \mu+s-\gamma \\ s+1 \end{pmatrix}}. \quad (2.40)$$

In Eqs. (2.39-2.40),

$$\begin{pmatrix} a \\ b \end{pmatrix} = \frac{a!\,(b-a)!}{b!} \quad (2.41)$$

designates the binomial coefficient.

2.3 Numerical Solution to the Radial Equation

Since analytical solutions to the radial Schrödinger equation are known for only a few central potentials, such as the Coulomb potential or the harmonic oscillator potential, it is necessary to resort to numerical methods to obtain solutions in practical cases.

We use finite difference techniques to find numerical solutions to the radial equation on a finite grid covering the region $r = 0$ to a *practical infinity*, a_∞, a point determined by requiring that $P(r)$ be negligible for $r > a_\infty$.

Near the origin, there are two solutions to the radial Schrödinger equation, the desired solution which behaves as $r^{\ell+1}$, and an irregular solution, referred to as the complementary solution, which diverges as $r^{-\ell}$ as $r \to 0$. Numerical errors near $r = 0$ introduce small admixtures of the complementary solution into the solution being sought. Integrating outward from the origin keeps such errors under control, since the complementary solution decreases in magnitude as r increases. In a similar way, in the asymptotic region, we integrate inward from a_∞ toward $r = 0$ to insure that errors from small admixtures of the complementary solution, which behaves as $e^{\lambda r}$ for large r, decrease as the integration proceeds from point to point. In summary, one expects the point-by-point numerical integration outward from $r = 0$ and inward from $r = \infty$ to yield solutions that are stable against small numerical errors.

The general procedure used to solve Eq.(2.13) is to integrate outward from the origin, using an appropriate point-by-point scheme, starting with solutions that are regular at the origin. The integration is continued to the outer *classical turning point*, the point beyond which classical motion in the potential $V(r) + \ell(\ell+1)/2r^2$ is impossible. In the region beyond the classical turning point, the equation is integrated inward, again using a point-by-point integration scheme, starting from $r = a_\infty$ with an approximate solution obtained from an asymptotic

series. Typically, we choose a_∞ so that the dimensionless quantity $\lambda r \approx 40$ for the first few steps of the inward integration. With this choice, $P(r)$ is roughly 10^{-12} of its maximum value near a_∞. The solutions from the inward and outward integrations are matched at the classical turning point. The energy is then adjusted until the derivative of $P(r)$ is continuous at the matching point.

The resulting function $P(r)$ is an eigenfunction and the corresponding energy E is its eigenvalue. To find a particular eigenfunction, we make use of the fact that different eigenfunctions have different numbers of nodes for $r > 0$. For a given value of ℓ, the lowest energy eigenfunction has no node, the next higher energy eigenfunction has one node, and so on. We first make a preliminary adjustment of the energy to obtain the desired number of nodes and then make a final fine adjustment to match the slope of the wave function at the classical turning point.

The radial wave function increases rapidly at small values of r then oscillates in the classically allowed region and gradually decreases beyond the classical turning point. To accommodate this behavior, it is convenient to adopt a nonuniform integration grid, more finely spaced at small r than at large r. Although there are many possible choices of grid, one that has proven to be both convenient and flexible is

$$\begin{array}{ll} r[i] = r_0\,(e^{t[i]} - 1)\,, & \text{where} \\ t[i] = (i-1)h\,, & i = 1, 2, \ldots, N\,. \end{array} \tag{2.42}$$

We typically choose $r_0 = 0.0005$ a.u., $h = 0.02 - 0.03$, and extend the grid to $N = 500$ points. These choices permit the radial Schrödinger equation to be integrated with high accuracy (parts in 10^{12}) for energies as low as 0.01 a.u..

We rewrite the radial Schrödinger equation as the equivalent pair of first order radial differential equations:

$$\frac{dP}{dr} = Q(r), \tag{2.43}$$

$$\frac{dQ}{dr} = -2\left(E - V(r) - \frac{\ell(\ell+1)}{2r^2}\right)P(r)\,. \tag{2.44}$$

On the uniformly-spaced t-grid, this pair of equations can be expressed as a single, two-component equation

$$\frac{dy}{dt} = f(y,t)\,, \tag{2.45}$$

where y is the array,

$$y(t) = \begin{bmatrix} P(r(t)) \\ Q(r(t)) \end{bmatrix}. \tag{2.46}$$

The two components of $f(y,t)$ are given by

$$f(y,t) = \frac{dr}{dt}\begin{bmatrix} Q(r(t)) \\ -2\left(E - V(r) - \dfrac{\ell(\ell+1)}{2r^2}\right)P(r(t)) \end{bmatrix}. \tag{2.47}$$

We can formally integrate Eq.(2.45) from one grid point, $t[n]$, to the next, $t[n+1]$, giving

$$y[n+1] = y[n] + \int_{t[n]}^{t[n+1]} f(y(t), t)\, dt\,. \tag{2.48}$$

2.3.1 Adams Method (ADAMS)

To derive the formula used in practice to carry out the numerical integration in Eq.(2.48), we introduce some notation from finite difference theory. More complete discussions of the calculus of difference operators can be found in textbooks on numerical methods such as Dahlberg and Björck (1974, chap. 7). Let the function $f(x)$ be given on a uniform grid and let $f[n] = f(x[n])$ be the value of $f(x)$ at the n^{th} grid point. We designate the backward difference operator by ∇:

$$\nabla f[n] = f[n] - f[n-1]\,. \tag{2.49}$$

Using this notation, $(1-\nabla)f_[n] = f[n-1]$. Inverting this equation, we may write,

$$\begin{array}{rcl} f[n+1] & = & (1-\nabla)^{-1} f[n], \\ f[n+2] & = & (1-\nabla)^{-2} f[n], \\ & \vdots & \end{array} \tag{2.50}$$

or more generally,

$$f[n+x] = (1-\nabla)^{-x} f[n]. \tag{2.51}$$

In these expressions, it is understood that the operators in parentheses are to be expanded in a power series in ∇, and that Eq.(2.49) is to be used iteratively to determine ∇^k .

Equation(2.51) is a general interpolation formula for equally spaced points. Expanding out a few terms, we obtain from Eq.(2.51)

$$\begin{array}{rcl} f[n+x] & = & \left(1 + \dfrac{x}{1!}\nabla + \dfrac{x(x+1)}{2!}\nabla^2 + \dfrac{x(x+1)(x+2)}{3!}\nabla^3 + \cdots\right) f[n]\,, \\ & = & \left(1 + x + \dfrac{x(x+1)}{2!} + \dfrac{x(x+1)(x+2)}{3!} + \cdots\right) f[n] \\ & - & \left(x + \dfrac{2x(x+1)}{2!} + \dfrac{3x(x+1)(x+2)}{3!} + \cdots\right) f[n-1] \\ & + & \left(\dfrac{x(x+1)}{2!} + \dfrac{3x(x+1)(x+2)}{3!} + \cdots\right) f[n-2] \\ & - & \left(\dfrac{x(x+1)(x+2)}{3!} + \cdots\right) f[n-3] + \cdots\,. \end{array} \tag{2.52}$$

Truncating this formula at the k^{th} term leads to a polynomial of degree k in x that passes through the points $f[n], f[n-1], \cdots, f[n-k]$, as x takes on the values $0, -1, -2, \cdots, -k$, respectively. We may use the interpolation formula

(2.51) to carry out the integration in Eq.(2.48), analytically leading to the result: (Adams-Bashforth)

$$\begin{aligned} y[n+1] &= y[n] - \frac{h\nabla}{(1-\nabla)\log(1-\nabla)} f[n] \,, \\ &= y[n] + h(1 + \frac{1}{2}\nabla + \frac{5}{12}\nabla^2 + \frac{9}{24}\nabla^3 + \cdots) f[n] \,. \end{aligned} \tag{2.53}$$

This equation may be rewritten, using the identity $(1-\nabla)^{-1} f[n] = f[n+1]$, as an interpolation formula: (Adams-Moulton)

$$\begin{aligned} y[n+1] &= y[n] - \frac{h\nabla}{\log(1-\nabla)} f[n+1] \,, \\ &= y[n] + h(1 - \frac{1}{2}\nabla - \frac{1}{12}\nabla^2 - \frac{1}{24}\nabla^3 + \cdots) f[n+1] \,. \end{aligned} \tag{2.54}$$

Keeping terms only to third-order and using Eqs.(2.53-2.54), we obtain the four-point (fifth-order) predict-correct formulas

$$\begin{aligned} y[n+1] &= y[n] + \frac{h}{24}(55f[n] - 59f[n-1] + 37f[n-2] - 9f[n-3]) \\ &\quad + \frac{251}{720} h^5 y^{(5)}[n] \,, \end{aligned} \tag{2.55}$$

$$\begin{aligned} y[n+1] &= y[n] + \frac{h}{24}(9f[n+1] + 19f[n] - 5f[n-1] + f[n-2]) \\ &\quad - \frac{19}{720} h^5 y^{(5)}[n] \,. \end{aligned} \tag{2.56}$$

The error terms in Eqs.(2.55-2.56) are obtained by evaluating the first neglected term in Eqs.(2.53-2.54) using the approximation

$$\nabla^k f[n] \approx h^k \left(\frac{d^k f}{dt^k} \right)[n] = h^k \left(\frac{d^{k+1} y}{dt^{k+1}} \right)[n] \,. \tag{2.57}$$

The magnitude of the error in Eq.(2.56) is smaller (by an order of magnitude) than that in Eq.(2.55), since interpolation is used in Eq.(2.56), while extrapolation is used in Eq.(2.55). Often, the less accurate extrapolation formula (2.55) is used to advance from point $t[n]$ (where $y[n]$, $f[n]$, $f[n-1]$, $f[n-2]$, and $f[n-3]$ are known) to the point $t[n+1]$. Using the predicted value of $y[n+1]$, one evaluates $f[n+1]$. The resulting value of $f[n+1]$ can then be used in the interpolation formula (2.56) to give a more accurate value for $y[n+1]$.

In our application of Adams method, we make use of the linearity of the differential equations (2.45) to avoid the extrapolation step altogether. To show how this is done, we first write the $k+1$ point Adams-Moulton interpolation formula from Eq.(2.54) in the form,

$$y[n+1] = y[n] + \frac{h}{D} \sum_{j=1}^{k+1} a[j]\, f[n-k+j] \,. \tag{2.58}$$

Table 2.1: Adams-Moulton integration coefficients

$a[1]$	$a[2]$	$a[3]$	$a[4]$	$a[5]$	$a[6]$	D	error
1	1					2	-1/12
-1	8	5				12	-1/24
1	-5	19	9			24	-19/720
-19	106	-264	646	251		720	-3/160
27	-173	482	-798	1427	475	1440	-863/60480

The coefficients $a[j]$ for 2-point to 7-point Adams-Moulton integration formulas are given in Table 2.1, along with the divisors D used in Eq.(2.58), and the coefficient of $h^{k+2}y^{(k+2)}[n]$ in the expression for the truncation error.

Setting $f(y,t) = G(t)y$, where G is a 2×2 matrix, we can take the $k+1$ term from the sum to the left-hand side of Eq.(2.58) to give

$$\left(1 - \frac{ha[k+1]}{D} G[n+1]\right) y[n+1] = y[n] + \frac{h}{D} \sum_{j=1}^{k} a[j]\, f[n-k+j]\,. \qquad (2.59)$$

From Eq.(2.47), it follows that G is an off-diagonal matrix of the form

$$G = \begin{pmatrix} 0 & b \\ c & 0 \end{pmatrix}\,, \qquad (2.60)$$

for the special case of the radial Schrödinger equation. The coefficients $b(t)$ and $c(t)$ can be read from Eq.(2.47):

$$b(t) = \tfrac{dr}{dt} \qquad c(t) = -2\tfrac{dr}{dt}\left(E - V(r) - \tfrac{\ell(\ell+1)}{2r^2}\right). \qquad (2.61)$$

The matrix

$$M[n+1] = 1 - \frac{ha[k+1]}{D}\, G[n+1]$$

on the left-hand side of Eq.(2.59) is readily inverted to give

$$M^{-1}[n+1] = \frac{1}{\Delta[n+1]} \begin{pmatrix} 1 & \lambda b[n+1] \\ \lambda c[n+1] & 1 \end{pmatrix}\,, \qquad (2.63)$$

where

$$\begin{aligned} \Delta[n+1] &= 1 - \lambda^2 b[n+1]c[n+1]\,, \\ \lambda &= \frac{ha[k+1]}{D}\,. \end{aligned}$$

Equation(2.59) is solved to give

$$y[n+1] = M^{-1}[n+1] \left(y[n] + \frac{h}{D} \sum_{j=1}^{k} a[j]\, f[n-k+j] \right)\,. \qquad (2.64)$$

This is the basic algorithm used to advance the solution to the radial Schrödinger equation from one point to the next. Using this equation, we achieve the accuracy of the predict-correct method without the necessity of separate predict and correct steps. To start the integration using Eq.(2.64), we must give initial values of the two-component function $f(t)$ at the points $1, 2, \cdots, k$. The subroutine ADAMS is designed to implement Eq.(2.64) for values of k ranging from 0 to 8.

2.3.2 Starting the Outward Integration (OUTSCH)

The k initial values of $y[j]$ required to start the outward integration using the $k+1$ point Adams method are obtained using a scheme based on Lagrangian differentiation formulas. These formulas are easily obtained from the basic finite difference expression for interpolation, Eq.(2.51). Differentiating this expression, we find

$$\left(\frac{dy}{dx}\right)[n-j] = -\log(1-\nabla)\,(1-\nabla)^j\, y[n]\,. \tag{2.65}$$

If Eq.(2.65) is expanded to k terms in a power series in ∇, and evaluated at the $k+1$ points, $j = 0, 1, 2, \cdots, k$, we obtain the $k+1$ point Lagrangian differentiation formulas. For example, with $k = 3$ and $n = 3$ we obtain the formulas:

$$\left(\frac{dy}{dt}\right)[0] = \frac{1}{6h}\left(-11y[0] + 18y[1] - 9y[2] + 2y[3]\right) - \frac{1}{4}h^3y^{(4)} \tag{2.66}$$

$$\left(\frac{dy}{dt}\right)[1] = \frac{1}{6h}\left(-2y[0] - 3y[1] + 6y[2] - y[3]\right) + \frac{1}{12}h^3y^{(4)} \tag{2.67}$$

$$\left(\frac{dy}{dt}\right)[2] = \frac{1}{6h}\left(y[0] - 6y[1] + 3y[2] + 2y[3]\right) - \frac{1}{12}h^3y^{(4)} \tag{2.68}$$

$$\left(\frac{dy}{dt}\right)[3] = \frac{1}{6h}\left(-2y[0] + 9y[1] - 18y[2] + 11y[3]\right) + \frac{1}{4}h^3y^{(4)}\,. \tag{2.69}$$

The error terms in Eqs.(2.66-2.69) are found by retaining the next higher-order differences in the expansion of Eq.(2.65) and using the approximation (2.57). Ignoring the error terms, we write the general $k+1$ point Lagrangian differentiation formula as

$$\left(\frac{dy}{dt}\right)[i] = \sum_{j=0}^{k} m[ij]\; y[j]\,, \tag{2.70}$$

where $i = 0, 1, \cdots, k$, and where the coefficients $m[ij]$ are determined from Eq.(2.65).

To find the values of $y[j]$ at the first few points along the radial grid, first we use the differentiation formulas (2.70) to eliminate the derivative terms from the differential equations at the points $j = 1, \cdots, k$, then we solve the resulting linear algebraic equations using standard methods.

Factoring $r^{\ell+1}$ from the radial wave function $P(r)$,

$$P(r) = r^{\ell+1}\, p(r)\,, \tag{2.71}$$

we may write the radial Schrödinger equation as

$$\frac{dp}{dt} = \frac{dr}{dt}\, q(t)\,, \tag{2.72}$$

$$\frac{dq}{dt} = -2\frac{dr}{dt}\left[(E - V(r))p(t) + \left(\frac{\ell+1}{r}\right) q(t)\right]\,. \tag{2.73}$$

Substituting for the derivatives from Eq.(2.70), we obtain the $2k \times 2k$ system of linear equations

$$\sum_{j=1}^{k} m[ij]\; p[j] - b[i]\; q[i] = -m[i0]\; p[0]\,, \tag{2.74}$$

$$\sum_{j=1}^{k} m[ij]\; q[j] - c[i]\; p[i] - d[i]\; q[i] = -m[i0]\; q[0]\,, \tag{2.75}$$

where

$$\begin{aligned} b(t) &= \frac{dr}{dt}\,, \\ c(t) &= -2\frac{dr}{dt}\left[E - V(r)\right]\,, \\ d(t) &= -2\frac{dr}{dt}\left(\frac{\ell+1}{r}\right)\,, \end{aligned} \tag{2.76}$$

and where $p[0]$ and $q[0]$ are the initial values of $p(t)$ and $q(t)$, respectively. If we assume that as $r \to 0$, the potential $V(r)$ is dominated by the nuclear Coulomb potential,

$$V(r) \to -\frac{Z}{r}\,, \tag{2.77}$$

then from Eq.(2.73) it follows that the initial values must be in the ratio

$$\frac{q[0]}{p[0]} = -\frac{Z}{\ell+1}\,. \tag{2.78}$$

We choose $p[0] = 1$ arbitrarily and determine $q[0]$ from Eq.(2.78).

The $2k \times 2k$ system of linear equations (2.74-2.75) are solved using standard methods to give $p[i]$ and $q[i]$ at the points $j = 1, \cdots, k$ along the radial grid. From these values we obtain

$$P[i] = r^{\ell+1}[i]\, p[i] \tag{2.79}$$

$$Q[i] = r^{\ell+1}[i]\left(q[i] + \frac{\ell+1}{r[i]}\, p[i]\right)\,. \tag{2.80}$$

These are the k initial values required to start the outward integration of the radial Schrödinger equation using the $k+1$ point Adams method. The routine OUTSCH implements the method described here to start the outward integration.

There are other ways to determine solutions to the second-order differential equations at the first k grid points. One obvious possibility is to use a power series representation for the radial wave function at small r. This method is not used since we must consider cases where the potential at small r is very different from the Coulomb potential and has no simple analytical structure. Such cases occur when we treat self-consistent fields or nuclear finite-size effects.

Another possibility is to start the outward integration using Runge-Kutta methods. Such methods require evaluation of the potential between the grid points. To obtain such values, for cases where the potential is not known analytically, requires additional interpolation. The present scheme is simple, accurate, and avoids such unnecessary interpolation.

2.3.3 Starting the Inward Integration (INSCH)

To start the inward integration using the $k+1$ point Adams method, we need k values of $P[i]$ and $Q[i]$ in the asymptotic region just preceding the practical infinity. We determine these values using an asymptotic expansion of the Schrödinger wave function. Let us suppose that the potential $V(r)$ in the asymptotic region, $r \approx a_\infty$, takes the limiting form,

$$V(r) \to -\frac{\zeta}{r}\,, \tag{2.81}$$

where ζ is the charge of the ion formed when one electron is removed. The radial Schrödinger equation in this region then becomes

$$\frac{dP}{dr} = Q(r), \tag{2.82}$$

$$\frac{dQ}{dr} = -2\left(E + \frac{\zeta}{r} - \frac{\ell(\ell+1)}{2r^2}\right)P(r)\,. \tag{2.83}$$

We seek an asymptotic expansion of $P(r)$ and $Q(r)$ of the form :

$$P(r) = r^\sigma e^{-\lambda r}\left\{a_0 + \frac{a_1}{r} + \cdots + \frac{a_k}{r^k} + \cdots\right\}\,, \tag{2.84}$$

$$Q(r) = r^\sigma e^{-\lambda r}\left\{b_0 + \frac{b_1}{r} + \cdots + \frac{b_k}{r^k} + \cdots\right\}\,. \tag{2.85}$$

Substituting the expansions (2.84-2.85) into the radial equations (2.82-2.83) and matching the coefficients of the two leading terms, we find that such an expansion is possible only if

$$\lambda = \sqrt{-2E}\,,$$

$$\sigma = \frac{\zeta}{\lambda}\,. \tag{2.86}$$

Using these values for λ and σ, the following recurrence relations for a_k and b_k are obtained by matching the coefficients of r^{-k} in Eqs.(2.82-2.83) :

$$a_k = \frac{\ell(\ell+1)-(\sigma-k)(\sigma-k+1)}{2k\lambda}\, a_{k-1}\,, \tag{2.87}$$

$$b_k = \frac{(\sigma+k)(\sigma-k+1)-\ell(\ell+1)}{2k}\, a_{k-1}\,. \tag{2.88}$$

We set $a_0 = 1$ arbitrarily, $b_0 = -\lambda$, and use Eqs.(2.87-2.88) to generate the coefficients of higher-order terms in the series. Near the practical infinity, the expansion parameter $2\lambda r$ is large (≈ 80), so relatively few terms in the expansion suffice to give highly accurate wave functions in this region. The asymptotic expansion is used to evaluate P_i and Q_i at the final k points on the radial grid. These values are used in turn to start a point-by-point inward integration to the classical turning point using the $k+1$ point Adams method. In the routine INSCH, the asymptotic series is used to obtain the values of $P(r)$ and $Q(r)$ at large r to start the inward integration using Adams method.

2.3.4 Eigenvalue Problem (MASTER)

To solve the eigenvalue problem, we:

1. Guess the energy E.
2. Use the routine OUTSCH to obtain values of the radial wave function at the first k grid points, and continue the integration to the outer classical turning point (a_c) using the routine ADAMS.
3. Use the routine INSCH to obtain the values of the wave function at the last k points on the grid, and continue the inward solution to a_c using the routine ADAMS.
4. Multiply the wave function and its derivative obtained in step 3 by a scale factor chosen to make the wave function for $r < a_c$ from step 2, and that for $r > a_c$ from step 3, continuous at $r = a_c$.

If the energy guessed in step 1 happened to be an energy eigenvalue, then not only the solution, but also its derivative, would be continuous at $r = a_c$. If it were the desired eigenvalue, then the wave function would also have the correct number of radial nodes, $n_r = n - \ell - 1$.

Generally the energy E in step 1 is just an estimate of the eigenvalue, so the numerical values determined by following steps 2 to 4 above give a wave function having an incorrect number of nodes and a discontinuous derivative at a_c. This is illustrated in Fig. 2.2. In the example shown there, we are seeking the $4p$ wave function in a Coulomb potential with $Z = 2$. The corresponding radial wave function should have $n_r = n - l - 1 = 2$ nodes. We start with the guess $E = -0.100$ a.u. for the energy and carry out steps 2 to 4 above. The resulting function, which is represented by the thin solid curve in the figure, has three nodes instead of two and has a discontinuous derivative at $a_c \approx 19$ a.u..

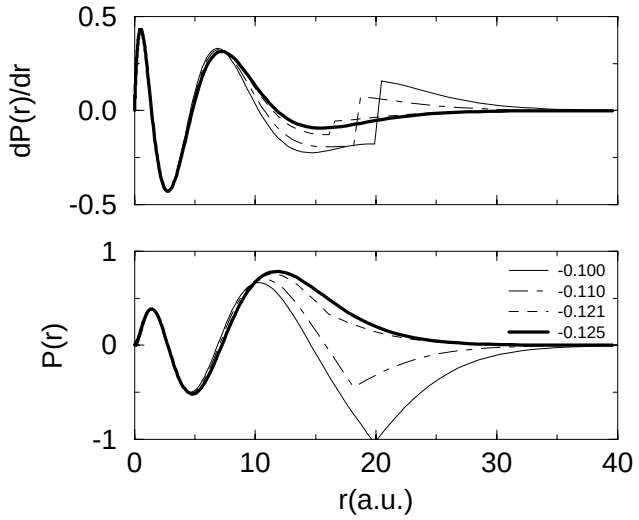

Figure 2.2: The radial wave function for a Coulomb potential with $Z = 2$ is shown at several steps in the iteration procedure leading to the $4p$ eigenstate.

The number of nodes increases with increasing energy. To reduce the number of nodes, we must, therefore, lower the energy. We do this by multiplying E (which is of course negative) by a factor of 1.1. Repeating steps 2 - 4 with $E = -0.110$ a.u., leads to the curve shown in the dot-dashed curve in the figure. The number of nodes remains $n_r = 3$, so we repeat the steps again with $E = 1.1(-0.110) = -0.121$ a.u.. At this energy, the number of nodes $n_r = 2$ is correct, as shown in the dashed curve in Fig. 2.2; however, the derivative of the wave function is still discontinuous at a_c. To achieve a wave function with a continuous derivative, we make further corrections to E using a perturbative approach.

If we let $P_1(r)$ and $Q_1(r)$ represent the radial wave function and its derivative at E_1, respectively, and let $P_2(r)$ and $Q_2(r)$ represent the same two quantities at E_2, then it follows from the radial Schrödinger equation that

$$\frac{d}{dr}(Q_2P_1 - P_2Q_1) = 2(E_1 - E_2)P_1P_2\,. \tag{2.89}$$

From this equation, we find that

$$2(E_1 - E_2)\int_{a_c}^{\infty} P_1\,P_2\,dr \;=\; -(Q_2P_1 - P_2Q_1)^+, \tag{2.90}$$

$$2(E_1 - E_2)\int_{0}^{a_c} P_1\,P_2\,dr \;=\; (Q_2P_1 - P_2Q_1)^-, \tag{2.91}$$

where the superscripts ± indicate that the quantities in parentheses are to be evaluated just above or just below a_c. These equations are combined to give

$$E_1 - E_2 = \frac{(Q_1^+ - Q_1^-)P_2(a_c) + (Q_2^- - Q_2^+)P_1(a_c)}{2\int_0^\infty P_1\, P_2\, dr}\,. \tag{2.92}$$

Suppose that the derivative Q_1 is discontinuous at a_c. If we demand that Q_2 be continuous at a_c, then the term $Q_2^- - Q_2^+$ in the numerator of (2.92) vanishes. Approximating P_2 by P_1 in this equation, we obtain

$$E_2 \approx E_1 + \frac{(Q_1^- - Q_1^+)P_1(a_c)}{2\int_0^\infty P_1^2\, dr}\,, \tag{2.93}$$

as an approximation for the eigenenergy. We use this approximation iteratively until the discontinuity in $Q(r)$ at $r = a_c$ is reduced to an insignificant level.

The program MASTER is designed to determine the wave function and the corresponding energy eigenvalue for specified values of n and ℓ by iteration. In this program, we construct an energy trap that reduces E (by a factor of 1.1) when there are too many nodes at a given step of the iteration, or increases E (by a factor of 0.9) when there are too few nodes. When the number of nodes is correct, the iteration is continued using Eq.(2.93) iteratively until the discontinuity in $Q(r)$ at $r = a_c$ is reduced to a negligible level. In the routine, we keep track of the least upper bound on the energy E_u (too many nodes) and the greatest lower bound E_l (too few nodes) as the iteration proceeds. If increasing the energy at a particular step of the iteration would lead to $E > E_u$, then we simply replace E by $(E+E_u)/2$, rather than following the above rules. Similarly, if decreasing E would lead to $E < E_l$, then we replace E by $(E + E_l)/2$.

For the example shown in the Fig. 2.2, it required 8 iterations to obtain the energy $E_{4p} = -1/8$ a.u. to 10 significant figures starting from the estimate $E = -.100$ a.u.. The resulting wave function is shown in the heavy solid line in the figure.

It is only necessary to normalize $P(r)$ and $Q(r)$ to obtain the desired radial wave function and its derivative. The normalization integral,

$$N^{-2} = \int_0^\infty P^2(r)dr\,,$$

is evaluated using the routine RINT; a routine based on the trapezoidal rule with endpoint corrections that will be discussed later. As a final step in the routine MASTER, the wave function and its derivative are multiplied by N to give a properly normalized numerical solution to the radial Schrödinger equation.

2.4 Potential Models

The potential experienced by a bound atomic electron near $r = 0$ is dominated by the nuclear Coulomb potential, so we expect

$$V(r) \approx -\frac{Z}{r},$$

for small r. At large r, on the other hand, an electron experiences a potential that is the sum of the attractive nuclear Coulomb potential and the sum of the repulsive potentials of the remaining electrons, so we expect

$$\lim_{r\to\infty} V(r) = -\frac{\zeta}{r},$$

with $\zeta = Z-N+1$ for an N electron atom with nuclear charge Z. The transition from a nuclear potential to an ionic potential is predicted by the Thomas-Fermi model, for example. However, it is possible to simply approximate the potential in the intermediate region by a smooth function of r depending on several parameters that interpolates between the two extremes. One adjusts the parameters in this potential to fit the observed energy spectrum as well as possible. We examine this approach in the following section.

2.4.1 Parametric Potentials

It is a simple matter to devise potentials that interpolate between the nuclear and ionic potentials. Two simple one-parameter potentials are:

$$V_a(r) = -\frac{Z}{r} + \frac{(Z-\zeta)\,r}{a^2+r^2}, \tag{2.94}$$

$$V_b(r) = -\frac{Z}{r} + \frac{Z-\zeta}{r}\,(1-e^{-r/b}). \tag{2.95}$$

The second term in each of these potentials approximates the electron-electron interaction. As an exercise, let us determine the values of the parameters a and b in Eqs.(2.94) and (2.95) that best represent the four lowest states ($3s, 3p, 4s$ and $3d$) in the sodium atom. For this purpose, we assume that the sodium spectrum can be approximated by that of a single valence electron moving in one of the above parametric potentials. We choose values of the parameters to minimize the sum of the squares of the differences between the observed levels and the corresponding numerical eigenvalues of the radial Schrödinger equation. To solve the radial Schrödinger equation, we use the routine MASTER described above. To carry out the minimization, we use the subroutine GOLDEN from the NUMERICAL RECIPES library. This routine uses the golden mean technique to find the minimum of a function of a single variable, taken to be the sum of the squares of the energy differences considered as a function of the parameter in the potential.

We find that the value $a = 0.2683$ a.u. minimizes the sum of the squares of the differences between the calculated and observed terms using the potential V_a from Eq.(2.94). Similarly, $b = 0.4072$ a.u. is the optimal value of the parameter in Eq.(2.95). In Table 2.2, we compare the observed sodium energy level with values calculated using the two potentials. It is seen that the calculated and observed levels agree to within a few percent for both potentials, although V_b leads to better agreement.

The electron-electron interaction potential for the two cases is shown in Fig. 2.3. These two potentials are completely different for $r < 1$ a.u., but agree

Table 2.2: Comparison of $n = 3$ and $n = 4$ levels (a.u.) of sodium calculated using parametric potentials with experiment.

State	V_a	V_b	Exp.
$3s$	-0.1919	-0.1881	-0.1889
$3p$	-0.1072	-0.1124	-0.1106
$4s$	-0.0720	-0.0717	-0.0716
$3d$	-0.0575	-0.0557	-0.0559

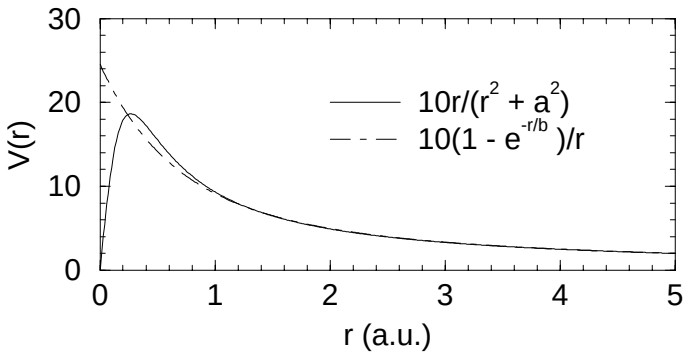

Figure 2.3: Electron interaction potentials from Eqs.(2.94) and (2.95) with parameters $a = 0.2683$ and $b = 0.4072$ chosen to fit the first four sodium energy levels.

closely for $r > 1$ a.u., where the $n = 3$ and $n = 4$ wave functions have their maxima.

Since the two potentials are quite different for small r, it is possible to decide which of the two is more reasonable by comparing predictions of levels that have their maximum amplitudes at small r with experiment. Therefore, we are led to compare the $1s$ energy from the two potentials with the experimentally measured $1s$ binding energy $E_{1s}^{\rm exp} = -39.4$ a.u. We find upon solving the radial Schrödinger equation that

$$E_{1s} = \begin{cases} -47.47\text{a.u.} & \text{for } V_a, \\ -40.14\text{a.u.} & \text{for } V_b. \end{cases}$$

It is seen that potential $V_b(r)$ predicts an energy that is within 2% of the experimental value, while V_a leads to a value of the $1s$ energy that disagrees with experiment by about 18%. As we will see later, theoretically determined potentials are closer to case b than to case a, as one might expect from the comparison here.

One can easily devise multi-parameter model potentials, with parameters adjusted to fit a number of levels precisely, and use the resulting wave functions to predict atomic properties. Such a procedure is a useful first step in examining the structure of an atom, but because of the *ad hoc* nature of the potentials being considered, it is difficult to assess errors in predictions made using such potentials.

2.4.2 Thomas-Fermi Potential

A simple approximation to the atomic potential was derived from a statistical model of the atom by L.H Thomas and independently by E. Fermi in 1927. This potential is known as the Thomas-Fermi potential. Although there has been a revival of research interest in the Thomas-Fermi method in recent years, we will consider only the most elementary version of the theory here to illustrate an *ab-initio* calculation of an atomic potential.

We suppose that bound electrons in an atom behave in the same way as free electrons confined to a box of volume V. For electrons in a box, the number of states d^3N available in a momentum range d^3p is given by

$$d^3N = 2\frac{V}{(2\pi)^3}d^3p, \tag{2.96}$$

where the factor 2 accounts for the two possible electron spin states. Assuming the box to be spherically symmetric, and assuming that all states up to momentum p_f (the Fermi momentum) are filled, it follows that the particle density ρ is

$$\rho = \frac{N}{V} = \frac{1}{\pi^2}\int_0^{p_f} p^2 dp = \frac{1}{3\pi^2}\, p_f^3. \tag{2.97}$$

Similarly, the kinetic energy density is given by

$$\epsilon_k = \frac{E_k}{V} = \frac{1}{\pi^2}\int_0^{p_f} \frac{p^2}{2}\, p^2 dp = \frac{1}{10\pi^2}\, p_f^5. \tag{2.98}$$

Using Eq.(2.97), we can express the kinetic energy density in terms of the particle density through the relation

$$\epsilon_k = \frac{3}{10}(3\pi^2)^{2/3}\rho^{5/3}\,. \tag{2.99}$$

In the Thomas-Fermi theory, it is assumed that this relation between the kinetic-energy density and the particle density holds not only for particles moving freely in a box, but also for bound electrons in the nonuniform field of an atom. In the atomic case, we assume that each electron experiences a spherically symmetric field and, therefore, that $\rho = \rho(r)$ is independent of direction.

The electron density $\rho(r)$ is assumed to vanish for $r \geq R$, where R is determined by requiring

$$\int_0^R 4\pi r'^2 \rho(r')dr' \; = N, \tag{2.100}$$

where N is the number of bound electrons in the atom.

In the Thomas-Fermi theory, the electronic potential is given by the classical potential of a spherically symmetric charge distribution:

$$V_e(r) = \int_0^R \frac{1}{r_>} 4\pi r'^2 \rho(r') dr' \,, \tag{2.101}$$

where $r_> = \max(r, r')$. The total energy of the atom in the Thomas-Fermi theory is obtained by combining Eq.(2.99) for the kinetic energy density with the classical expressions for the electron-nucleus potential energy and the electron-electron potential energy to give the following semi-classical expression for the energy of the atom:

$$E = \int_0^R \left\{ \frac{3}{10}(3\pi^2)^{2/3}\rho^{2/3} - \frac{Z}{r} + \frac{1}{2}\int_0^R \frac{1}{r_>} 4\pi r'^2 \rho(r') dr' \right\} 4\pi r^2 \rho(r) dr \,. \tag{2.102}$$

The density is determined from a variational principle; the energy is required to be a minimum with respect to variations of the density, with the constraint that the number of electrons is N. Introducing a Lagrange multiplier λ, the variational principal $\delta(E - \lambda N) = 0$ can be written

$$\int_0^R \left\{ \frac{1}{2}(3\pi^2)^{2/3}\rho^{2/3} - \frac{Z}{r} + \int_0^R \frac{1}{r_>} 4\pi r'^2 \rho(r') dr' - \lambda \right\} 4\pi r^2 \delta\rho(r) dr = 0. \tag{2.103}$$

Requiring that this condition be satisfied for arbitrary variations $\delta\rho(r)$ leads to the following integral equation for $\rho(r)$:

$$\frac{1}{2}(3\pi^2)^{2/3}\rho^{2/3} - \frac{Z}{r} + \int_0^R \frac{1}{r_>} 4\pi r'^2 \rho(r') dr' = \lambda \,. \tag{2.104}$$

Evaluating this equation at the point $r = R$, where $\rho(R) = 0$, we obtain

$$\lambda = -\frac{Z}{R} + \frac{1}{R}\int_0^R 4\pi r'^2 \rho(r') dr' = -\frac{Z - N}{R} = V(R) \,, \tag{2.105}$$

where $V(r)$ is the sum of the nuclear and atomic potentials at r. Combining (2.105) and (2.104) leads to the relation between the density and potential,

$$\frac{1}{2}(3\pi^2)^{2/3}\rho^{2/3} = V(R) - V(r) \,. \tag{2.106}$$

Since $V(r)$ is a spherically symmetric potential obtained from purely classical arguments, it satisfies the radial Laplace equation,

$$\frac{1}{r}\frac{d^2}{dr^2} r V(r) = -4\pi\rho(r) \,, \tag{2.107}$$

which can be rewritten

$$\frac{1}{r}\frac{d^2}{dr^2} r[V(R) - V(r)] = 4\pi\rho(r) \,. \tag{2.108}$$

Substituting for $\rho(r)$ from (2.106) leads to

$$\frac{d^2}{dr^2} r[V(R) - V(r)] = \frac{8\sqrt{2}}{3\pi} \frac{(r[V(R) - V(r)])^{3/2}}{r^{1/2}} . \tag{2.109}$$

It is convenient to change variables to ϕ and x, where

$$\phi(r) = \frac{r[V(R) - V(r)]}{Z} , \tag{2.110}$$

and

$$x = r/\xi , \tag{2.111}$$

with

$$\xi = \left(\frac{9\pi^2}{128Z} \right)^{1/3} . \tag{2.112}$$

With the aid of this transformation, we can rewrite the *Thomas-Fermi equation* (2.109) in dimensionless form:

$$\frac{d^2\phi}{dx^2} = \frac{\phi^{3/2}}{x^{1/2}} . \tag{2.113}$$

Since $\lim_{r\to 0} r[V(r) - V(R)] = -Z$, the desired solution to (2.113) satisfies the boundary condition $\phi(0) = 1$. From $\rho(R) = 0$, it follows that $\phi(X) = 0$ at $X = R/\xi$.

By choosing the initial slope appropriately, we can find solutions to the Thomas-Fermi equation that satisfy the two boundary conditions for a wide range of values X. The correct value of X is found by requiring that the normalization condition (2.100) is satisfied. To determine the point X, we write Eq.(2.108) as

$$r\frac{d^2\phi}{dr^2} = \frac{1}{Z} 4\pi r^2 \rho(r) . \tag{2.114}$$

From this equation, it follows that $N(r)$, the number of electrons inside a sphere of radius r, is given by

$$\frac{N(r)}{Z} = \int_0^r r \frac{d^2\phi(r)}{dr^2} dr \tag{2.115}$$

$$= \left(r\frac{d\phi}{dr} - \phi \right)_0^r \tag{2.116}$$

$$= r\frac{d\phi}{dr} - \phi(r) + 1 . \tag{2.117}$$

Evaluating this expression at $r = R$, we obtain the normalization condition

$$X \left(\frac{d\phi}{dx} \right)_X = -\frac{Z - N}{Z} . \tag{2.118}$$

An iterative scheme is set up to solve the Thomas-Fermi differential equation. First, two initial values of X are guessed: $X = X_a$ and $X = X_b$. The

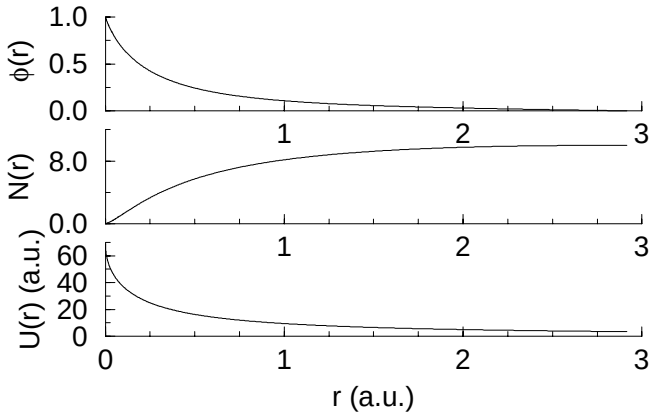

Figure 2.4: Thomas-Fermi functions for the sodium ion, $Z = 11$, $N = 10$. Upper panel: the Thomas-Fermi function $\phi(r)$. Center panel: $N(r)$, the number of electrons inside a sphere of radius r. Lower panel: $U(r)$, the electron contribution to the potential.

Thomas-Fermi equation (2.113) is integrated inward to $r = 0$ twice: the first time starting at $x = X_a$, using initial conditions $\phi(X_a) = 0$, $d\phi/dx(X_a) = -(Z - N)/X_a Z$, and the second time starting at $x = X_b$, using initial conditions $\phi(X_b) = 0$, $d\phi/dx(X_b) = -(Z - N)/X_b Z$. We examine the quantities $\phi(0) - 1$ in the two cases. Let us designate this quantity by f; thus, f_a is the value of $\phi(0) - 1$ for the first case, where initial conditions are imposed at $x = X_a$, and f_b is the value of $\phi(0) - 1$ in the second case. If the product $f_a f_b > 0$, we choose two new points and repeat the above steps until $f_a f_b < 0$. If $f_a f_b < 0$, then it follows that the correct value of X is somewhere in the interval between X_a and X_b. Assuming that we have located such an interval, we continue the iteration by interval halving: choose $X = (X_a + X_b)/2$ and integrate inward, test the sign of $f f_a$ and $f f_b$ to determine which subinterval contains X and repeat the above averaging procedure. This interval halving is continued until $|f| < \epsilon$, where ϵ is a tolerance parameter. The value chosen for ϵ determines how well the boundary condition at $x = 0$ is to be satisfied.

In the routine THOMAS, we use the fifth-order Runge-Kutta integration scheme given in Abramowitz and Stegun to solve the Thomas-Fermi equation. We illustrate the solution obtained for the sodium ion, $Z = 11, N = 10$ in Fig. 2.4. The value of R obtained on convergence was $R = 2.914$ a.u.. In the top panel, we show $\phi(r)$ in the interval 0 - R. In the second panel, we show the corresponding value of $N(r)$, the number of electrons inside a sphere of radius r. In the bottom panel, we give the electron contribution to the potential. Comparing with Fig. 2.3, we see that the electron-electron potential $U(r)$ from the Thomas-Fermi potential has the same general shape as the electron-

interaction contribution to the parametric potential $V_b(r)$. This is consistent with the previous observation that $V_b(r)$ led to an accurate inner-shell energy for sodium.

2.5 Separation of Variables for Dirac Equation

To describe the fine structure of atomic states from first principles, it is necessary to treat the bound electrons relativistically. In the independent particle picture, this is done by replacing the one-electron Schrödinger orbital $\psi(\mathbf{r})$ by the corresponding Dirac orbital $\varphi(\mathbf{r})$. The orbital $\varphi(\mathbf{r})$ satisfies the single-particle Dirac equation

$$h_D\varphi = E\varphi, \tag{2.119}$$

where h_D is the Dirac Hamiltonian. In atomic units, h_D is given by

$$h_D = c\boldsymbol{\alpha}\cdot\boldsymbol{p} + \beta c^2 + V(r)\,. \tag{2.120}$$

The constant c is the speed of light; in atomic units, $c = 137.0359895\ldots$. The quantities $\boldsymbol{\alpha}$ and β in Eq.(2.120) are 4×4 Dirac matrices:

$$\boldsymbol{\alpha} = \begin{pmatrix} 0 & \boldsymbol{\sigma} \\ \boldsymbol{\sigma} & 0 \end{pmatrix}, \quad \beta = \begin{pmatrix} 1 & 0 \\ 0 & -1 \end{pmatrix}. \tag{2.121}$$

The 2×2 matrix $\boldsymbol{\sigma}$ is the Pauli spin matrix, discussed in Sec. 1.2.1.

The total angular momentum is given by $\mathbf{J} = \mathbf{L} + \mathbf{S}$, where $\mathbf{L}$ is the orbital angular momentum, and $\mathbf{S}$ is the 4×4 spin angular momentum matrix,

$$\mathbf{S} = \frac{1}{2}\begin{pmatrix} \boldsymbol{\sigma} & 0 \\ 0 & \boldsymbol{\sigma} \end{pmatrix}. \tag{2.122}$$

It is not difficult to show that $\mathbf{J}$ commutes with the Dirac Hamiltonian. We may, therefore, classify the eigenstates of h_D according to the eigenvalues of energy, J^2 and J_z .The eigenstates of J^2 and J_z are easily constructed using the two-component representation of $\boldsymbol{S}$. They are the spherical spinors $\Omega_{\kappa m}(\hat{r})$.

If we seek a solution to the Dirac equation (2.120) having the form

$$\varphi_\kappa(\mathbf{r}) = \frac{1}{r}\begin{pmatrix} iP_\kappa(r) & \Omega_{\kappa m}(\hat{r}) \\ Q_\kappa(r) & \Omega_{-\kappa m}(\hat{r}) \end{pmatrix}, \tag{2.123}$$

then we find, with the help of the identities (1.124, 1.126), that the radial functions $P_\kappa(r)$ and $Q_\kappa(r)$ satisfy the coupled first-order differential equations:

$$(V + c^2)\,P_\kappa + c\left(\frac{d}{dr} - \frac{\kappa}{r}\right)Q_\kappa = EP_\kappa \tag{2.124}$$

$$-c\left(\frac{d}{dr} + \frac{\kappa}{r}\right)P_\kappa + (V - c^2)\,Q_\kappa = EQ_\kappa \tag{2.125}$$

where $V(r) = V_{nuc}(r)+U(r)$. The normalization condition for the orbital $\varphi_\kappa(\mathbf{r})$,

$$\int \varphi_\kappa^\dagger(\mathbf{r})\varphi_\kappa(\mathbf{r})d^3r = 1, \tag{2.126}$$

can be written

$$\int_0^\infty [\, P_\kappa^2(r) + Q_\kappa^2(r)\,]dr = 1, \tag{2.127}$$

when expressed in terms of the radial functions $P_\kappa(r)$ and $Q_\kappa(r)$. The radial eigenfunctions and their associated eigenvalues, E, can be determined analytically for a Coulomb potential. In practical cases, however, the eigenvalue problem must be solved numerically.

2.6 Radial Dirac Equation for a Coulomb Field

In this section, we seek analytical solutions to the radial Dirac equations (2.124) and (2.125) for the special case $V(r) = -Z/r$. As a first step in our analysis, we examine these equations at large values of r. Retaining only dominant terms as $r \to \infty$, we find

$$c\frac{dQ_\kappa}{dr} = (E - c^2)P_\kappa\,, \tag{2.128}$$

$$c\frac{dP_\kappa}{dr} = -(E + c^2)Q_\kappa\,. \tag{2.129}$$

This pair of equations can be converted into the second-order equation

$$c^2\frac{d^2P_\kappa}{dr^2} + (E^2 - c^4)P_\kappa = 0, \tag{2.130}$$

which has two linearly independent solutions, $e^{\pm\lambda r}$, with $\lambda = \sqrt{c^2 - E^2/c^2}$. The physically acceptable solution is

$$P_\kappa(r) = e^{-\lambda r}\,. \tag{2.131}$$

The corresponding solution Q_κ is given by

$$Q_\kappa(r) = \sqrt{\frac{c^2 - E}{c^2 + E}}e^{-\lambda r}. \tag{2.132}$$

Factoring the asymptotic behavior, we express the radial functions in the form

$$P_\kappa = \sqrt{1 + E/c^2}e^{-\lambda r}(F_1 + F_2)\,, \tag{2.133}$$

$$Q_\kappa = \sqrt{1 - E/c^2}e^{-\lambda r}(F_1 - F_2)\,. \tag{2.134}$$

Substituting this *ansatz* into (2.124) and (2.125), we find that the functions F_1 and F_2 satisfy the coupled equations

$$\frac{dF_1}{dx} = \frac{EZ}{c^2\lambda x}F_1 + \left(\frac{Z}{\lambda x} - \frac{\kappa}{x}\right)F_2\,, \tag{2.135}$$

$$\frac{dF_2}{dx} = -\left(\frac{Z}{\lambda x} + \frac{\kappa}{x}\right)F_1 + \left(1 - \frac{EZ}{c^2\lambda x}\right)F_2\,, \tag{2.136}$$

where $x = 2\lambda r$.

We seek solutions to Eqs.(2.135,2.136) that have the limiting forms $F_1 = a_1 x^\gamma$ and $F_2 = a_2 x^\gamma$ as $x \to 0$. Substituting these expressions into (2.135) and (2.136) and retaining only the most singular terms, we find:

$$\frac{a_2}{a_1} = \frac{\gamma - EZ/c^2\lambda}{-\kappa + Z/\lambda} = \frac{-\kappa - Z/\lambda}{\gamma + EZ/c^2\lambda}. \tag{2.137}$$

Clearing fractions in the right-hand equality, leads to the result $\gamma^2 = \kappa^2 - Z^2/c^2 = \kappa^2 - \alpha^2 Z^2$. Here, we have used the fact that $c = 1/\alpha$ in atomic units. The physically acceptable value of γ is given by the positive square root, $\gamma = \sqrt{\kappa^2 - \alpha^2 Z^2}$. Next, we use Eq.(2.135) to express F_2 in terms of F_1,

$$F_2 = \frac{1}{-\kappa + Z/\lambda}\left[x\frac{dF_1}{dx} - \frac{EZ}{c^2\lambda}F_1\right]. \tag{2.138}$$

This equation, in turn, can be used to eliminate F_2 from Eq.(2.136), leading to

$$x\frac{d^2F_1}{dx^2} + (1-x)\frac{dF_1}{dx} - \left(\frac{\gamma^2}{x^2} - \frac{EZ}{c^2\lambda}\right)F_1 = 0\,. \tag{2.139}$$

Finally, we write

$$F_1(x) = x^\gamma F(x)\,, \tag{2.140}$$

and find that the function $F(x)$ satisfies the Kummer's equation,

$$x\frac{d^2F}{dx^2} + (b-x)\frac{dF}{dx} - aF = 0\,, \tag{2.141}$$

where $a = \gamma - EZ/c^2\lambda$, and $b = 2\gamma + 1$. This equation is identical to Eq.(2.18) except for the values of the parameters a and b. The solutions to Eq.(2.141) that are regular at the origin are the Confluent Hypergeometric functions written out in Eq.(2.19). Therefore,

$$F_1(x) = x^\gamma\, F(a,b,x)\,. \tag{2.142}$$

The function $F_2(x)$ can also be expressed in terms of Confluent Hypergeometric functions. Using Eq.(2.138), we find

$$F_2(x) = \frac{x^\gamma}{(-\kappa + Z/\lambda)}\left(x\frac{dF}{dx} + aF\right) = \frac{(\gamma - EZ/c^2\lambda)}{(-\kappa + Z/\lambda)}x^\gamma F(a+1,b,x)\,. \tag{2.143}$$

Combining these results, we obtain the following expressions for the radial Dirac functions:

$$\begin{aligned} P_\kappa(r) &= \sqrt{1+E/c^2}\,e^{-x/2}x^\gamma[(-\kappa+Z/\lambda)F(a,b,x) \\ &\quad +(\gamma - EZ/c^2\lambda)F(a+1,b,x)\big], \end{aligned} \tag{2.144}$$

$$\begin{aligned} Q_\kappa(r) &= \sqrt{1-E/c^2}\,e^{-x/2}x^\gamma[(-\kappa+Z/\lambda)F(a,b,x) \\ &\quad -(\gamma - EZ/c^2\lambda)F(a+1,b,x)\big]. \end{aligned} \tag{2.145}$$

These solutions have yet to be normalized.

We now turn to the eigenvalue problem. First, we examine the behavior of the radial functions at large r. We find:

$$F(a,b,x) \rightarrow \frac{\Gamma(b)}{\Gamma(a)}\, e^x x^{a-b}[1+O(|x|^{-1})]\,, \tag{2.146}$$

$$aF(a+1,b,x) \rightarrow \frac{\Gamma(b)}{\Gamma(a)}\, e^x x^{a+1-b}[1+O(|x|^{-1})]\,. \tag{2.147}$$

From these equations, it follows that the radial wave functions are normalizable if, and only if, the coefficients of the exponentials in Eqs.(2.146) and (2.147) vanish. As in the nonrelativistic case, this occurs when $a = -n_r$, where $n_r = 0, -1, -2, \cdots$. We define the principal quantum number n through the relation, $n = k + n_r$, where $k = |\kappa| = j + 1/2$. The eigenvalue equation, therefore, can be written

$$EZ/c^2\lambda = \gamma + n - k\,.$$

The case $a = -n_r = 0$ requires special attention. In this case, one can solve the eigenvalue equation to find $k = Z/\lambda$. From this, it follows that the two factors $-\kappa + Z/\lambda$ and $\gamma - EZ/c^2\lambda$ in Eqs.(2.144) and (2.145) vanish for $\kappa = k > 0$. States with $n_r = 0$ occur only for $\kappa < 0$. Therefore, for a given value of $n > 0$ there are $2n-1$ possible eigenfunctions: n eigenfunctions with $\kappa = -1, -2, \cdots - n$, and $n-1$ eigenfunctions with $\kappa = 1, 2, \cdots n-1$.

Solving the eigenvalue equation for E, we obtain

$$E_{n\kappa} = \frac{c^2}{\sqrt{1 + \frac{\alpha^2 Z^2}{(\gamma+n-k)^2}}}\,. \tag{2.148}$$

It is interesting to note that the Dirac energy levels depend only on $k = |\kappa|$. Those levels having the same values of n and j, but different values of ℓ are degenerate. Thus, for example, the $2s_{1/2}$ and $2p_{1/2}$ levels in hydrogenlike ions are degenerate. By contrast, levels with the same value of n and ℓ but different values of j, such as the $2p_{1/2}$ and $2p_{3/2}$ levels, have different energies. The separation between two such levels is called the fine-structure interval.

Expanding (2.148) in powers of αZ, we find

$$E_{n\kappa} = c^2 - \frac{Z^2}{2n^2} - \frac{\alpha^2 Z^4}{2n^3}\left(\frac{1}{k} - \frac{3}{4n}\right) + \cdots\,. \tag{2.149}$$

The first term in this expansion is just the electron's rest energy (mc^2) expressed in atomic units. The second term is precisely the nonrelativistic Coulomb-field binding energy. The third term is the leading fine-structure correction. The fine-structure energy difference between the $2p_{3/2}$ and $2p_{1/2}$ levels in hydrogen is predicted by this formula to be

$$\Delta E_{2p} = \frac{\alpha^2}{32}\,\text{a.u.} = 0.3652\,\text{cm}^{-1}\,,$$

in close agreement with the measured separation. The separation of the $2s_{1/2}$ and $2p_{1/2}$ levels in hydrogen is measured to be $0.0354\,\mathrm{cm}^{-1}$. The degeneracy between these two levels predicted by the Dirac equation is lifted by the Lamb-shift!

Let us introduce the (noninteger) parameter $N = Z/\lambda = (\gamma + n - k)c^2/E$. From (2.148), we find $N = \sqrt{n^2 - 2(n-k)(k-\gamma)}$. Thus, $N = n$ when $n = k$. With this definition, the coefficients of the hypergeometric functions in Eqs.(2.144) and (2.145) can be written

$$(-\kappa + Z/\lambda) = (N - \kappa)\,, \tag{2.150}$$

$$(\gamma - EZ/c^2\lambda) = -(n-k)\,. \tag{2.151}$$

Introducing the normalization factor

$$N_{n\kappa} = \frac{1}{N\,\Gamma(2\gamma+1)}\sqrt{\frac{Z\,\Gamma(2\gamma+1+n-k)}{2\,(n-k)!\,(N-\kappa)}}\,, \tag{2.152}$$

we can write the radial Dirac Coulomb wave functions as

$$\begin{aligned} P_{n\kappa}(r) &= \sqrt{1+E_{n\kappa}/c^2}\,N_{n\kappa}e^{-x/2}x^{\gamma}\,[(N-\kappa)F(-n+k,2\gamma+1,x) \\ &\quad -(n-k)F(-n+k+1,2\gamma+1,x)]\,, \end{aligned} \tag{2.153}$$

$$\begin{aligned} Q_{n\kappa}(r) &= \sqrt{1-E_{n\kappa}/c^2}\,N_{n\kappa}e^{-x/2}x^{\gamma}\,[(N-\kappa)F(-n+k,2\gamma+1,x) \\ &\quad +(n-k)F(-n+k+1,2\gamma+1,x)]\,. \end{aligned} \tag{2.154}$$

These functions satisfy the normalization condition (2.127). It should be noticed that the ratio of the scale factors in (2.153) and (2.154) is $\sqrt{(1-E_{n\kappa}/c^2)/(1+E_{n\kappa}/c^2)} \approx \alpha Z/2n$. Thus, $Q_{n\kappa}(r)$ is several orders of magnitude smaller than $P_{n\kappa}(r)$ for $Z = 1$. For this reason, $P_{n\kappa}$ and $Q_{n\kappa}$ are referred to as the large and small components of the radial Dirac wave function, respectively.

As a specific example, let us consider the $1s_{1/2}$ ground state of an electron in a hydrogenlike ion with nuclear charge Z. For this state, $n = 1$, $\kappa = -1$, $k = 1$, $\gamma = \sqrt{1-\alpha^2Z^2}$, $E_{n\kappa}/c^2 = \gamma$, $N = 1$, $\lambda = Z$ and $x = 2Zr$. Therefore,

$$P_{1-1}(r) = \sqrt{\frac{1+\gamma}{2}}\sqrt{\frac{2Z}{\Gamma(2\gamma+1)}}\,(2Zr)^{\gamma}e^{-Zr}\,,$$

$$Q_{1-1}(r) = \sqrt{\frac{1-\gamma}{2}}\sqrt{\frac{2Z}{\Gamma(2\gamma+1)}}\,(2Zr)^{\gamma}e^{-Zr}\,.$$

In Fig. 2.5, we plot the $n = 2$ Coulomb wave functions for nuclear charge $Z = 2$. The small components $Q_{2\kappa}(r)$ in the figure are scaled up by a factor of $1/\alpha Z$ to make them comparable in size to the large components $P_{2\kappa}(r)$. The large components are seen to be very similar to the corresponding nonrelativistic Coulomb wave functions $P_{n\ell}(r)$, illustrated in Fig. 2.1. The number of nodes in the $P_{n\kappa}(r)$ is $n - \ell - 1$. The number of nodes in $Q_{n\kappa}(r)$ is also $n - \ell - 1$

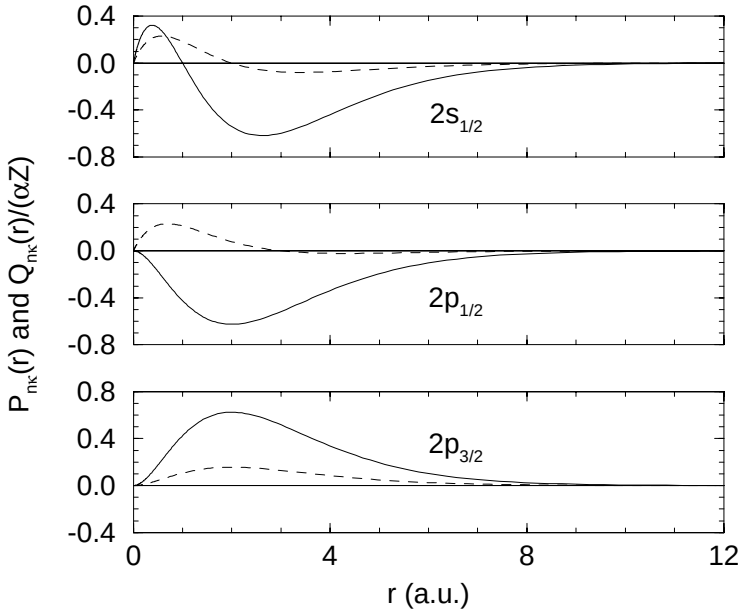

Figure 2.5: Radial Dirac Coulomb wave functions for the $n = 2$ states of hydrogenlike helium, $Z = 2$. The solid lines represent the large components $P_{2\kappa}(r)$ and the dashed lines represent the scaled small components, $Q_{2\kappa}(r)/\alpha Z$.

for $\kappa < 0$, but is $n - \ell$ for $\kappa > 0$. These rules for the nodes will be useful in designing a numerical eigenvalue routine for the Dirac equation. It should be noticed that, except for sign, the large components of the $2p_{1/2}$ and $2p_{3/2}$ radial wave functions are virtually indistinguishable.

2.7 Numerical Solution to Dirac Equation

The numerical treatment of the radial Dirac equation closely parallels that used previously to solve the radial Schrödinger equation. The basic point-by-point integration of the radial equations is performed using the Adams-Moulton scheme (ADAMS). We obtain the values of the radial functions near the origin necessary to start the outward integration using an algorithm based on Lagrangian differentiation (OUTDIR). The corresponding values of the radial functions near the practical infinity, needed to start the inward integration, are obtained from an asymptotic expansion of the radial functions (INDIR). A scheme following the pattern of the nonrelativistic routine MASTER is then used to solve the eigenvalue problem. In the paragraphs below we describe the modifications of the nonrelativistic routines that are needed in the Dirac case.

To make comparison with nonrelativistic calculations easier, we subtract the rest energy c^2 a.u. from E_κ in our numerical calculations. In the sequel, we use $W_\kappa = E_\kappa - c^2$ instead of E as the value of the energy in the relativistic case.

The choice of radial grid is identical to that used in the nonrelativistic case; $r(t)$ gives the value of the distance coordinate on the uniformly-spaced t grid. The radial Dirac equations on the t grid take the form

$$\frac{dy}{dt} = f(y,t)\,, \tag{2.155}$$

where $y(t)$ and $f(y,t)$ are the two-component arrays:

$$y = \begin{pmatrix} P_\kappa \\ Q_\kappa \end{pmatrix}\,, \tag{2.156}$$

$$f(y,t) = r' \begin{pmatrix} -(\kappa/r)\,P_\kappa(r) - \alpha[W_\kappa - V(r) + 2\alpha^{-2}]Q_\kappa(r) \\ (\kappa/r)\,Q_\kappa(r) + \alpha[W_\kappa - V(r)]P_\kappa(r) \end{pmatrix}\,, \tag{2.157}$$

where, $r'(t) = \frac{dr}{dt}$.

2.7.1 Outward and Inward Integrations (ADAMS, OUTDIR, INDIR)

ADAMS: We integrate Eqs.(2.156) and(2.157) forward using the Adams-Moulton algorithm given in Eq.(2.58):

$$y[n+1] = y[n] + \frac{h}{D}\sum_{j=1}^{k+1} a[j]\,f[n-k+j]\,. \tag{2.158}$$

The coefficients $a[j]$ and D for this integration formula are given in Table 2.1. Writing $f(y,t) = G(t)\,y$, equation (2.158) can be put in the form (2.59),

$$\left(1 - \frac{ha[k+1]}{D}G[n+1]\right) y[n+1] = y[n] + \frac{h}{D}\sum_{j=1}^{k} a[j]\,f[n-k+j]\,, \tag{2.159}$$

where G is the 2×2 matrix

$$G(t) = \begin{pmatrix} a(t) & b(t) \\ c(t) & d(t) \end{pmatrix}\,, \tag{2.160}$$

with

$$\begin{aligned} a(t) &= -r'\,(\kappa/r)\,, & b(t) &= -\alpha\,r'\,(W_\kappa - V(r) + 2\alpha^{-2})\,, \\ c(t) &= \alpha\,r'\,(W_\kappa - V(r))\,, & d(t) &= r'\,(\kappa/r)\,. \end{aligned} \tag{2.161}$$

The matrix $M[n+1] = 1 - \frac{ha[k+1]}{D}G[n+1]$ on the left-hand side of Eq.(2.160) can be inverted to give

$$M^{-1}[n+1] = \frac{1}{\Delta[n+1]} \begin{pmatrix} 1 - \lambda d[n+1] & \lambda b[n+1] \\ \lambda c[n+1] & 1 - \lambda a[n+1] \end{pmatrix}\,, \tag{2.162}$$

where

$$\begin{aligned}\Delta[n+1] &= 1-\lambda^2(b[n+1]c[n+1]-a[n+1]d[n+1])\,,\\ \lambda &= \frac{ha[k+1]}{D}\,.\end{aligned}$$

With these definitions, the radial Dirac equation can be written in precisely the same form as the radial Schrödinger equation (2.64)

$$y[n+1]=M^{-1}[n+1]\left(y[n]+\frac{h}{D}\sum_{j=1}^{k}a[j]\,f[n-k+j]\right)\,. \tag{2.163}$$

This formula is used in the relativistic version of the routine ADAMS to carry out the step-by-step integration of the Dirac equation.

As in the nonrelativistic case, we must supply values of y_n at the first k grid points. This is done by adapting the procedure used to start the outward integration of the Schrödinger equation to the Dirac case.

OUTDIR: The values of y_n at the first k grid points, needed to start the outward integration using (2.163), are obtained using Lagrangian integration formulas. As a preliminary step, we factor r^γ from the radial functions $P_\kappa(r)$ and $Q_\kappa(r)$, where $\gamma=\sqrt{k^2-(\alpha Z)^2}$. We write:

$$P_\kappa(r) = r^\gamma u(r(t)), \tag{2.164}$$
$$Q_\kappa(r) = r^\gamma v(r(t)), \tag{2.165}$$

and find,

$$du/dt = a(t)u(t)+b(t)v(t), \tag{2.166}$$
$$dv/dt = c(t)u(t)+d(t)v(t), \tag{2.167}$$

where,

$$a(t) = -(\gamma+\kappa)r'/r, \tag{2.168}$$
$$b(t) = -\alpha(W-V(r)+2\alpha^{-2})r', \tag{2.169}$$
$$c(t) = \alpha(W-V(r))r', \tag{2.170}$$
$$d(t) = -(\gamma-\kappa)r'/r. \tag{2.171}$$

We normalize our solution so that, at the origin, $u_0=u(0)=1$. It follows that $v_0=v(0)$ takes the value

$$v_0 = -(\kappa+\gamma)/\alpha Z, \quad \text{for } \kappa>0, \tag{2.172}$$
$$= \alpha Z/(\gamma-\kappa), \qquad \text{for } \kappa<0, \tag{2.173}$$

provided the potential satisfies

$$V(r)\to -\frac{Z}{r},$$

as $r \to 0$. The two equations (2.172) and (2.173) lead to identical results mathematically; however, (2.172) is used for $\kappa > 0$ and (2.173) for $\kappa < 0$ to avoid unnecessary loss of significant figures by cancellation for small values of αZ. One can express du/dt and dv/dt at the points $t[i]$, $i = 0, 1, \cdots, k$ in terms of $u[i] = u(t[i])$ and $v[i] = v(t[i])$ using the Lagrangian differentiation formulas written down in Eq.(2.70). The differential equations thereby become inhomogeneous matrix equations giving the vectors $(u[1], u[2], \cdots, u[k])$ and $(v[1], v[2], \cdots, v[k])$ in terms of initial values $u[0]$ and $v[0]$:

$$\sum_{j=1}^{k} m[ij]\ u[j] - a[i]\ u[i] - b[i]\ v[i] = -m[i0]\ u[0], \tag{2.174}$$

$$\sum_{j=1}^{k} m[ij]\ v[j] - c[i]\ u[i] - d[i]\ v[i] = -m[i0]\ v[0]. \tag{2.175}$$

This system of $2k \times 2k$ inhomogeneous linear equations can be solved by standard routines to give $u[i]$ and $v[i]$ at the points $i = 1, 2, \cdots, k$. The corresponding values of P_κ and Q_κ are given by

$$P_\kappa(r[i]) = r[i]^\gamma\ u[i], \tag{2.176}$$

$$Q_\kappa(r[i]) = r[i]^\gamma\ v[i]. \tag{2.177}$$

These equations are used in the routine OUTDIR to give the k values required to start the outward integration using a $k+1$-point Adams-Moulton scheme.

INDIR: The inward integration is started using an asymptotic expansion of the radial Dirac functions. The expansion is carried out for r so large that the potential $V(r)$ takes on its asymptotic form

$$V(r) = -\frac{\zeta}{r},$$

where $\zeta = Z - N + 1$ is the ionic charge of the atom. We assume that the asymptotic expansion of the radial Dirac functions takes the form

$$P_\kappa(r) = r^\sigma e^{-\lambda r} \left\{ \sqrt{\frac{c^2+E}{2c^2}} \left[1 + \frac{a_1}{r} + \frac{a_2}{r} + \cdots\right] + \sqrt{\frac{c^2-E}{2c^2}} \left[\frac{b_1}{r} + \frac{b_2}{r} + \cdots\right] \right\}, \tag{2.178}$$

$$Q_\kappa(r) = r^\sigma e^{-\lambda r} \left\{ \sqrt{\frac{c^2+E}{2c^2}} \left[1 + \frac{a_1}{r} + \frac{a_2}{r} + \cdots\right] - \sqrt{\frac{c^2-E}{2c^2}} \left[\frac{b_1}{r} + \frac{b_2}{r} + \cdots\right] \right\}, \tag{2.179}$$

where $\lambda = \sqrt{c^2 - E^2/c^2}$. The radial Dirac equations admit such a solution only if $\sigma = E\zeta/c^2\lambda$. The expansion coefficients can be shown to satisfy the following recursion relations:

$$b_1 = \frac{1}{2c}\left(\kappa + \frac{\zeta}{\lambda}\right), \tag{2.180}$$

$$b_{n+1} = \frac{1}{2n\lambda}\left(\kappa^2 - (n-\sigma)^2 - \frac{\zeta^2}{c^2}\right) b_n\,, \quad n = 1, 2, \cdots, \tag{2.181}$$

$$a_n = \frac{c}{n\lambda}\left(\kappa + (n-\sigma)\frac{E}{c^2} - \frac{\zeta\lambda}{c^2}\right) b_n\,, \quad n = 1, 2, \cdots. \tag{2.182}$$

In the routine INDIR, Eqs.(2.178) and (2.179) are used to generate the k values of $P_\kappa(r)$ and $Q_\kappa(r)$ needed to start the inward integration.

2.7.2 Eigenvalue Problem for Dirac Equation (MASTER)

The method that we use to determine the eigenfunctions and eigenvalues of the radial Dirac equation is a modification of that used in the nonrelativistic routine MASTER to solve the eigenvalue problem for the Schrödinger equation. We guess an energy, integrate the equation outward to the outer classical turning point a_c using OUTDIR, integrate inward from the practical infinity a_∞ to a_c using INDIR and, finally, scale the solution in the region $r > a_c$ so that the large component $P(r)$ is continuous at a_c. A preliminary adjustment of the energy is made to obtain the correct number of nodes ($= n - l - 1$) for $P(r)$ by adjusting the energy upward or downward as necessary. At this point we have a continuous large component function $P(r)$ with the correct number of radial nodes; however, the small component $Q(r)$ is discontinuous at $r = a_c$. A fine adjustment of the energy is made using perturbation theory to remove this discontinuity.

If we let $P_1(r)$ and $Q_1(r)$ be solutions to the radial Dirac equation corresponding to energy W_1 and let $P_2(r)$ and $Q_2(r)$ be solutions corresponding to energy W_2, then it follows from the radial Dirac equations that

$$\frac{d}{dr}(P_1Q_2 - P_2Q_1) = \frac{1}{c}(W_2 - W_1)(P_1P_2 + Q_1Q_2)\,. \tag{2.183}$$

Integrating both sides of this equation from 0 to a_c and adding the corresponding integral of both sides from a_c to infinity, we obtain the identity

$$P_1(a_c)(Q_2^- - Q_2^+) + P_2(a_c)(Q_1^+ - Q_1^-) = \frac{1}{c}(W_2 - W_1)\int_0^\infty (P_1P_2 + Q_1Q_2)dr\,, \tag{2.184}$$

where Q_1^+ and Q_2^+ are the values of the small components at a_c obtained from inward integration, and Q_1^- and Q_2^- are the values at a_c obtained from outward integration. If we suppose that Q_1 is discontinuous at a_c and if we require that Q_2 be continuous, then we obtain from (2.184) on approximating $P_2(r)$ and $Q_2(r)$ by $P_1(r)$ and $Q_1(r)$,

$$W_2 \approx W_1 + \frac{cP_1(a_c)(Q_1^+ - Q_1^-)}{\int_0^\infty (P_1^2 + Q_1^2)dr}\,. \tag{2.185}$$

Table 2.3: Parameters for the Tietz and Green potentials.

	Tietz		Green	
Element	t	γ	H	d
Rb	1.9530	0.2700	3.4811	0.7855
Cs	2.0453	0.2445	4.4691	0.8967
Au	2.4310	0.3500	4.4560	0.7160
Tl	2.3537	0.3895	4.4530	0.7234

The approximation (2.185) is used iteratively to reduce the discontinuity in $Q(r)$ at $r = a_c$ to insignificance. The Dirac eigenvalue routine DMASTER is written following the pattern of the nonrelativistic eigenvalue routine MASTER, incorporating the routines OUTDIR and INDIR to carry out the point-by-point integration of the radial equations and using the approximation (2.185) to refine the solution.

2.7.3 Examples using Parametric Potentials

As in the nonrelativistic case, it is possible to devise parametric potentials to approximate the effects of the electron-electron interaction. Two potentials that have been used with some success to describe properties of large atoms having one valence electron are the Tietz potential

$$V(r) = -\frac{1}{r}\left[1 + \frac{(Z-1)e^{-\gamma r}}{(1+tr)^2}\right], \tag{2.186}$$

and the Green potential

$$V(r) = -\frac{1}{r}\left[1 + \frac{Z-1}{H(e^{r/d}-1)+1}\right]. \tag{2.187}$$

Each of these potentials contain two parameters that can be adjusted to fit experimentally measured energy levels. In Table 2.3, we list values of the parameters for rubidium (Z=37), cesium (Z=55), gold (Z=79) and thallium (Z=81). Energies of low-lying states of these atoms obtained by solving the Dirac equation in the two potentials are listed in Table 2.4. Wave functions obtained by solving the Dirac equation in parametric potentials have been successfully employed to predict properties of heavy atoms (such as hyperfine constants) and to describe the interaction of atoms with electromagnetic fields. The obvious disadvantage of treating atoms using parametric potentials is that there is no *a priori* reason to believe that properties, other than those used as input data in the fitting procedure, will be predicted accurately. In the next chapter, we take up the Hartree-Fock theory, which provides an *ab-initio* method for calculating electronic potentials, atomic energy levels and wave functions.

Table 2.4: Energies obtained using the Tietz and Green potentials.

State	Tietz	Green	Exp.	State	Tietz	Green	Exp.
Rubidium $Z = 37$				Cesium $Z = 55$			
$5s_{1/2}$	-0.15414	-0.15348	-0.15351	$6s_{1/2}$	-0.14343	-0.14312	-0.14310
$5p_{1/2}$	-0.09557	-0.09615	-0.09619	$6p_{1/2}$	-0.09247	-0.09224	-0.09217
$5p_{3/2}$	-0.09398	-0.09480	-0.09511	$6p_{3/2}$	-0.08892	-0.08916	-0.08964
$6s_{1/2}$	-0.06140	-0.06215	-0.06177	$7s_{1/2}$	-0.05827	-0.05902	-0.05865
$6p_{1/2}$	-0.04505	-0.04570	-0.04545	$7p_{1/2}$	-0.04379	-0.04424	-0.04393
$6p_{3/2}$	-0.04456	-0.04526	-0.04510	$7p_{3/2}$	-0.04270	-0.04323	-0.04310
$7s_{1/2}$	-0.03345	-0.03382	-0.03362	$8s_{1/2}$	-0.03213	-0.03251	-0.03230
Gold $Z = 79$				Thallium $Z = 81$			
$6s_{1/2}$	-0.37106	-0.37006	-0.33904	$6p_{1/2}$	-0.22456	-0.22453	-0.22446
$6p_{1/2}$	-0.18709	-0.17134	-0.16882	$6p_{3/2}$	-0.18320	-0.17644	-0.18896
$6p_{3/2}$	-0.15907	-0.14423	-0.15143	$7s_{1/2}$	-0.10195	-0.10183	-0.10382
$7s_{1/2}$	-0.09386	-0.09270	-0.09079	$7p_{1/2}$	-0.06933	-0.06958	-0.06882
$7p_{1/2}$	-0.06441	-0.06313	-0.06551	$7p_{3/2}$	-0.06391	-0.06374	-0.06426
$7p_{3/2}$	-0.05990	-0.05834	-0.06234	$8s_{1/2}$	-0.04756	-0.04771	-0.04792
$8s_{1/2}$	-0.04499	-0.04476	-0.04405	$8p_{1/2}$	-0.03626	-0.03639	-0.03598

Bibliography

H. A. Bethe and E. E. Salpeter. *Quantum Mechanics of One- and Two-Electron Atoms*. Academic Press, New York, 1957.

G. Dahlberg and Å. Björck. *Numerical Methods*. Prentice Hall, New York, 1974.

W. Magnus and F. Oberhettinger. *Formulas and Theorems for the Functions of Mathematical Physics*. Chelsea, New York, 1949.